2D Materials

OPEN ACCESS

RECEIVED
11 December 2017

REVISED
8 March 2018

ACCEPTED FOR PUBLICATION
27 March 2018

PUBLISHED
27 April 2018

PAPER

Impact of graphene oxide on human placental trophoblast viability, functionality and barrier integrity

Melanie Kucki[1,4], Leonie Aengenheister[1,4], Liliane Diener[1], Alexandra V Rippl[1], Sandra Vranic[2], Leon Newman[2], Ester Vazquez[3], Kostas Kostarelos[2], Peter Wick[1] and Tina Buerki-Thurnherr[1]

[1] Laboratory for Particles-Biology Interactions, Empa—Swiss Federal Laboratories for Materials Science and Technology, Lerchenfeldstrasse 5, CH-9014 St. Gallen, Switzerland
[2] Nanomedicine Laboratory, Faculty of Medical & Human Sciences and National Graphene Institute, University of Manchester, M13 9PT, Manchester, United Kingdom
[3] Departamento de Química Orgánica, Facultad de Ciencias y Tecnologías Químicas-IRICA, Universidad de Castilla-LaMancha, Av. Camilo Jose Cela, 10—13071 Ciudad Real, Spain
[4] Contributed equally to this paper.

E-mail: mel.kucki@gmx.de, leonie.aengenheister@empa.ch, liliane.diener@empa.ch, alexandra.rippl@empa.ch, sandra.vranic@manchester.ac.uk, leon.newman@manchester.ac.uk, ester.vazquez@uclm.es, kostas.kostarelos@manchester.ac.uk, peter.wick@empa.ch and tina.buerki@empa.ch

Keywords: graphene oxide, placenta barrier, nanosafety, barrier integrity

Supplementary material for this article is available online

Abstract

Graphene oxide (GO) is considered a promising 2D material for biomedical applications. However, the biological health effects of GO are not yet fully understood, in particular for highly sensitive populations such as pregnant women and their unborn children. Especially the potential impact of GO on the human placenta, a transient and multifunctional organ that enables successful pregnancy, has not been investigated yet. Here we performed a mechanistic *in vitro* study on the placental uptake and biological effects of four non-labelled GO with varying physicochemical properties using the human trophoblast cell line BeWo. No overt cytotoxicity was observed for all GO materials after 48 h of exposure at concentrations up to 40 μg ml^{-1}. However, exposure to GO materials induced a slight decrease in mitochondrial activity and human choriogonadotropin secretion. In addition, GO induced a transient opening of the trophoblast barrier as evidenced by a temporary increase in the translocation of sodium fluorescein, a marker molecule for passive transport. Evidence for cellular uptake of GO was found by transmission electron microscopy analysis, revealing uptake of even large micro-sized GO by BeWo cells. Although GO did not elicit major acute adverse effects on BeWo trophoblast cells, the pronounced cellular internalization as well as the potential adverse effects on hormone release and barrier integrity warrants further studies on the long-term consequences of GO on placental functionality in order to understand potential embryo-fetotoxic risks.

Introduction

Nanomaterials have attracted great attention as candidates for nanomedical applications, e.g. as contrast agents and drug nanocarriers [1]. Targeted drug delivery using nanoparticles (NPs) offers the possibility to deliver drugs to specific cells and tissues which increases efficacy and enables to minimize undesired side effects of the drug. Nevertheless, concerns have been raised regarding potential adverse effects of NPs entering the blood stream, especially for sensitive populations including pregnant women and developing fetus. In the recent years it has been shown that several NPs can cross the placental barrier in dependence of the particle properties (e.g. size) and surface modifications but the underlying transfer mechanisms are only poorly investigated and understood [2, 3]. But even in the absence of placental translocation NPs may induce placental damage, thereby causing potential indirect embryo-fetotoxicity [4–8].

Graphene-related materials (GRM) and other 2D materials have recently attracted a lot of interest in respect to nano- and biomedical application [9–18]. Especially water dispersible graphene oxide (GO) is under investigation as potential drug delivery platform

[19]. Due to the sheet character of 2D materials GO exhibits a large surface area for attachment of targeting ligands and allows facile functionalization. Nevertheless, effects of GO exposure need to be understood before considering its biomedical application. While some *in vitro* studies report negative acute effects on exposed cells, others found no cytotoxicity [20–22], as reviewed by Kiew *et al* [23]. A recent study in mice has demonstrated rapid clearance of GO from the blood stream after intravenous application [10]. Nevertheless, GO has the potential to reach the placenta in significant amounts as this is a highly perfused organ that is extensively exposed to circulating substances.

To date the impact of 2D-materials on the human placental barrier has not been investigated yet (*in vitro*, *in vivo*, *ex vivo*). However, a profound knowledge on the impact of GO at the placental barrier is required for the safe design of GO materials for medical or consumer applications in pregnancy. For other members of the carbon family such as single-walled and multi-walled carbon nanotubes, indirect and direct fetotoxic effects were found in animal studies [5, 24–26]. Xu *et al* investigated the potential impact of rGO on mice and pregnancy after injection of rGO via the tail vein. Female mice exposed to rGO before pregnancy or in early gestational stage (~6 d) gave birth to mostly healthy offspring, but some malformed mouse fetuses were observed after injection of rGO at early gestational phase. Furthermore, injection of rGO in late gestational phase (~20 d) led to abortions as well as death of the mothers dependent on the applied rGO concentration [27]. Xu *et al* assumed that there was no transfer of small rGO from the circulation of the dam to the fetus, but that a negative effect on the mother's health resulted in indirect fetotoxic effects [27]. These studies indicate that GRM bear the potential to exhibit negative (direct or indirect) effects on pregnancy, placental homeostasis and function, as well as on the developing fetus.

Nevertheless, it should be noted that the results from animal studies cannot be directly extrapolated to humans as the placenta is the most species-specific organ with unique structure and function [28–30].

In brief, the human placenta develops during pregnancy in order to meet the changing needs of the growing fetus. The placental barrier separating the maternal and fetal blood stream is composed of four layers when matured: a multinucleated, single layered syncytiotrophoblast (ST), a mononucleated but multilayered cytotrophoblast (CT), and the fetal stroma containing fibroblasts, macrophages and the endothelial cells of the fetal capillaries. While the ST is non-proliferative, the CT cells propagate and replenish the ST layer. As pregnancy progresses, the materno-fetal exchange is enhanced due to a significant reduction of the placental barrier thickness from 10 μm in the first trimester to 2–5 μm at term [2]. The reduced thickness is due to the thinning of the ST, a morphological change of the CT's phenotype and its partial disappearance and the migration of fetal capillaries closer to the basal lamina [2, 31, 32].

The aim of the here presented study was to explore the potential influence of label-free GO materials with distinct physicochemical properties on viability and function of human trophoblasts, which constitutes the first and rate-limiting cell layer of the placental barrier. For this purpose we applied a well-established 2D cell culture model, namely the human choriocarcinoma cell line BeWo (b30 clone). The BeWo cell line exhibits several characteristics of human trophoblasts *in vivo* including the production of placental hormones such as human choriogonadotropin (hCG) [33–35], and the b30 clone can form a tight monolayer if cultivated on a microporous membrane [36, 37]. Acute toxicity studies were performed including impact of GO on cell viability, barrier integrity, hormone production and cellular uptake. Only non-labelled GO samples were applied to prevent any artefacts derived from functionalization with linkers and labelling agents which bear the potential to alter cellular uptake behaviour.

Materials and methods

Graphene-related materials (GRM) and physicochemical characterization

Graphene oxide 1 (GO1) was obtained from Cheap Tubes (Battleboro, 112 Mercury Drive, VT05301, USA; www.cheaptubes.com). GO4 was provided by Grupo Antolin, Spain. GO1 and GO4 were characterized as described in Kucki *et al* [21].

Graphite flakes (Graflake 9580) were obtained from Nacional Grafite Ltd (Brazil) and used for the preparation of large and small graphene oxide (l-GO (f3) and s-GO (f3)). Graphene oxide sheets were synthesized using the modified Hummers method previously described [38, 39]. Briefly, 0.8 g of graphite flakes was mixed with 0.4 g of sodium nitrate in a round-bottom flask, and then 18.4 ml of sulfuric acid 99.999% was added slowly to the mixture. After a homogenized mixture was obtained, 2.4 g of potassium permanganate was slowly added and the mixture was maintained for 30 min. Next, 37 ml of water for injection was added dropwise due to the violent exothermic reaction, and the temperature was continuously monitored and kept at 98 °C for 30 min. The mixture was further diluted with 112 ml of water for injection, and 30% hydrogen peroxide was added for the reduction of the residual potassium permanganate, manganese dioxide, and manganese heptoxide to soluble manganese sulfate salts. The resulting mixture was purified by several centrifugation steps at 9000 rpm for 20 min until a viscous orange/brown layer of pure GO started to appear on top of the oxidation by-products at neutral pH. Obtained GO gel-like layer was extracted carefully with warm water, resulting in the large GO. Final concentrations ranging between 1 and 2 mg ml^{-1} were obtained with a yield of ca. 10%. l-GO was freeze-dried, reconstituted in water for injection, sonicated

in a bath sonicator (VWR, 80W) for 5 min, and centrifuged at 13 000 rpm for 5 min at room temperature to prepare the s-GO. Structural properties such as lateral dimension and thickness of the GO materials have been studied by optical microscopy, TEM, and AFM.

Transmission electron microscopy (TEM)

TEM was performed using a FEI Tecnai 12 Biotwin mi-croscope (FEI, The Netherlands) at an acceleration voltage of 100 kV. Images were taken with Gatan Orius SC1000 CCD camera (GATAN, UK). One drop of sample was placed on a Formvar/carbon-coated copper grid. Filter paper was used to remove the excess material.

Atomic force microscopy (AFM)

A multimode AFM was used on the tapping-mode with a J-type scanner, Nanoscope V8 controller (Veeco, Cambridge, UK), and an OTESPA silicon probe (Bruker, UK). Images were taken in air by depositing 20 μl of 100 μg ml^{-1} of GO on a freshly cleaved mica surface (Agar Scientific, Essex, UK) coated with poly-l-lysine 0.01% (Sigma-Aldrich, UK) and allowed to adsorb for 5 min. Excess unbound material was removed by washing with Milli-Q water and then allowed to dry in air; this step was repeated once. Lateral dimension and thickness distributions of GO were carried out using NanoScope Analysis software (version 1.40 Bruker, UK).

Endotoxin detection

s-GO and l-GO were produced following the recently described protocol for the production of endotoxin-free GO [22]. All applied GO samples were tested for potential endotoxin contamination by LAL Gel Clot Assay (PyrogentPlus™, Lonza, Walkersville, USA; Assay sensitivity: 0.03 EU ml^{-1}) and Endosafe®PTS portable test system (PTS100, Charles River Laboratories, Charleston, USA). Endotoxin detection of GO4 was already performed and reported by Mukherjee *et al* [22], designated as GO-C. The LAL Gel Clot Assay was performed according to [40]. Control standard endotoxin (CSE) from *Escherichia coli* O55:B5 served as positive control. LAL Reagent water (Lonza; <0.005 EU/ml) was applied as negative control. GO stock dispersions with a concentration of 1 mg ml^{-1} GO in LAL reagent water were prepared and diluted in a two-fold dilution series. Each GO sample was tested at minimum three different GO concentrations with two replicates each. Tests were repeated with an independent dilution series. In case of negative results GO samples were tested for assay interference according to [40]. Endosafe®PTS Assay was performed with Endosafe®PTS Cartridges (Charles River Laboratories, Charleston, USA) with an assay sensitivity of 0.01 EU/ml. Tests were performed according to the manufacturer's instructions and results were considered as valid when the acceptance criteria given by the manufacturer were fulfilled (sample coefficient variation and LPS spike coefficient variation both < 25%, LPS spike recovery 50–200%).

Cell culture

Human trophoblast cell line BeWo b30 Aberdeen was kindly provided by Prof Dr Ursula Graf-Hausner (Zurich University of Applied Sciences, Wädenswil, Switzerland) with permission of Dr Alan L Schwartz (Washington University School of Medicine, MO, USA). BeWo cells were cultivated in Ham's F-12K (Kaighn's) medium (Gibco, Paisley, UK) supplemented with 10% fetal calf serum (FCS, Invitrogen, Basel, Switzerland), 1% L-Glutamine (Gibco, Luzern, Switzerland) and 1% penicillin–streptomycin–neomycin (PSN, Gibco, Luzern, Switzerland) and incubated in humidified atmosphere with 5% CO_2 at 37 °C. Cells were routinely sub-cultured twice a week at 70%–80% confluence by 0.5% trypsin-EDTA (Sigma, Buchs, Switzerland) treatment.

GO dispersion

GO1 and GO4 powder were dispersed in ultra-pure water (MilliporeQ, endotoxin values <0.03 EU/ml, determined with LAL Gel Clot Assay) under sterile conditions to a stock concentration of 1 mg ml^{-1} GO. GO1 and GO4 dispersions were treated by ultra-sonication (bath sonication; Bandelin Sonorex SUPER RK 156 BH) for 60 s to eliminate visible GO aggregates. s-GO and l-GO were already obtained in aqueous dispersion and stored at room temperature and protected from light until further use. s-GO and l-GO were likewise diluted in ultra-pure water to a concentration of 1 mg ml^{-1} GO. For exposure experiments GO dispersions were diluted in supplemented cell culture medium (Ham's F-12K (Kaighn's) medium supplemented with 10% FCS, 1% L-Glutamine and 1% PSN) to the final applied GO concentrations.

Cell viability

Metabolic activity of BeWo cells after exposure to GO was assessed by MTS (3-(4,5-dimethylthiazol-2-yl)-5-(3-carboxymethoxyphenyl)-2-(4-sulfophenyl)-2H-tetrazolium, inner salt) assay (CellTiter 96® AQueous One Solution Cell Proliferation Assay, Promega Corporation, Madison, USA). The MTS assay was performed according to the manufacturer's instructions with slight changes to consider intrinsic GO absorbance as described in Kucki *et al* [21]. In short BeWo cells (Passage 20-29) were seeded in 96-well plates with a seeding density of 1×10^4 cells/well ($\sim 3.1 \times 10^4$ cells cm^{-2}) and incubated overnight at standard cell culture conditions. Cells were exposed to GO (0–40 μg GO/ml; 0–25 μg GO/cm^2 growth area; 100 μl per well) for 24 and 48 h. Unexposed BeWo cells were used as negative controls. Cells exposed to cadmium sulphate ($CdSO_4$, 0–1000 μM, Sigma-Aldrich, Buchs, Switzerland) were applied as positive control. The supernatant was replaced by addition of

120 μl working solution (20 μl MTS reagent plus 100 μl phenol red-free RPMI-1640 medium). Background absorbance (t0 value) was immediately measured at 490 nm wavelength to consider the intrinsic absorbance of residual substrate- or cell associated GO. Final absorbance (t1 value) was measured at 490 nm wavelengths after incubation in humidified atmosphere with 5% CO_2 at 37 °C for 60 min. Final absorbance values (t1 values) were corrected well-to-well for intrinsic GO absorbance by subtraction of the background (t0 values). Data is presented as mean (M) and standard deviation (SD) of at least three independent experiments with three replicates per sample.

Determination of the total cell number of adherent BeWo cells by modified lactate dehydrogenase (LDH) assay

Total number of adherent cells was assessed as described in Kucki *et al* [21] by application of the CytoTox96® Non-Radioactive Cytotoxicity Assay (Promega Corporation, Madison, USA). BeWo cells were seeded in 96-well plates with a density of 1×10^4 cells/well and incubated overnight at standard cell culture conditions. After exposure to either GO (0–40 μg ml^{-1} GO), GO-free medium (negative control) or medium with cadmium sulphate ($CdSO_4$, 0–1000 μM, positive control) for 48 h, cells were washed twice with pre-warmed phosphate buffered saline (PBS) and incubated in lysis solution (9% Triton-X 100, Sigma-Aldrich, Buchs, Switzerland) for 45 min at 37 °C. Background absorbance (t0 value) at 490 nm wavelength was measured to consider the intrinsic absorbance of residual substrate-or cell-associated GO. After addition of the assay reagent lysed cells were incubated for 30 min at room temperature (RT). Stop solution was added to terminate the assay reaction and final absorbance (t1 value) was measured at 490 nm wavelength. Results were corrected well-to-well for intrinsic GO absorbance (t1 − t0). Data is presented as mean (M) and standard deviation (SD) of at least three independent experiments with three replicates for each sample.

β-hCG Elisa

To investigate the influence of GO exposure on β-hCG production BeWo cells were seeded in 96-well plates at a density of 3000 cells/well in 100 μl supplemented medium. For each sample and control four replicates were applied. Cells were incubated for 48 h under standard cell culture conditions. To induce differentiation cells were thereafter incubated in fresh medium containing 20 μM forskolin (Sigma, Buchs, Switzerland) for 24 h under standard cell culture conditions. In parallel control cells were incubated in medium without forskolin to assess whether GO exposure can induce cell differentiation. Thereafter cells were exposed to GO (5-40 μg ml^{-1}; 100 μl per well) for 24 h in the absence of forskolin. Supernatants of the respective four replicates were pooled and stored at −80 °C until further use. Quantification of the β-hCG production was performed by β-hCG ELISA. High protein binding 96 well plates (Corning) were pre-coated with capture antibody (rabbit anti-human chorionic gonadotropin, 1:1000 in 50 mM $NaHCO_3$ A0231, Dako, Denmark) overnight at 4 °C. Plates were rinsed thrice with wash buffer (0.1% Tween 20 in PBS, Sigma-Aldrich, Buchs, Switzerland), followed by blocking with 0.5% BSA (Sigma-Aldrich, Buchs, Switzerland) in PBS for 2 h at RT in a humidified chamber. After washing thrice with wash buffer samples and β-hCG standard dilutions were added to the wells and incubated 1.5 h at 37 °C. Thereafter wells were washed thrice and detection antibody (mouse anti-human chorionic gonadotropin IgG1, 1:5000, in 1 % BSA in PBS, MCA 1436, Biorad, Cressier, Switzerland) was added. Plates were incubated for 1.5 h at 37 °C. Afterwards wells were rinsed five times with wash buffer followed by addition of the secondary detection antibody (goat anti-mouse IgG HRP, 1:5000 diluted in 1% BSA in PBS, 100 μl/well, Biorad, Cressier, Switzerland) and incubation at 37 °C for 1.5 h. Wells were rinsed five times with wash buffer prior addition of HRP substrate solution. After incubation at room temperature for 15 min absorbance was measured at 370 nm wavelength with a microplate reader (Mithras^2 LB 943 Monochromator Multimode Reader, Berthold Technologies GmbH, Zug, Switzerland). β-hCG values were calculated by application of a β-hCG standard series with linearity between 0–30 mIU/ml.

Scanning electron microscopy (SEM)

For SEM analysis BeWo cells were either seeded on clean and sterile cover glasses (15 mm Ø, Menzel GmbH, Braunschweig, Germany) in 12-well cell culture plates or on Transwell® membranes (Corning®, 12-well, pore size 3.0 μm, growth area 1.12 cm^2, polycarbonate (PC), Sigma-Aldrich, Buchs, Switzerland). BeWo cells were seeded at a density of 1×10^5 cell per well and incubated for 24 h to allow cell attachment. Cell cultures were exposed to either 20 μg ml^{-1} or 40 μg ml^{-1} GO in supplemented Ham's F-12K medium for 24 h in parallel to control cells without GO exposure. Cells were washed twice in pre-warmed phosphate buffered saline (PBS) and fixed by addition of modified Karnovsky fixation solution (4 g paraformaldehyde (PFA, CAS 30525-89-4), 50 ml aqua bidest, 5 ml glutaraldehyde 50% (GA, CAS 111-30-8), 45 ml phosphate buffered saline without glucose with pH 7.4). Fixation was performed for 1 h at room temperature under a fume hood followed by two washing steps with PBS. Dehydration was performed by ascending ethanol series (50%–100% ethanol) and final addition of hexamethyldisilizane (HMDS, CAS 999-97-3). Samples were dried overnight in a fume hood and stored in a desiccator until further use. Before coating glass slides and cut-out Transwell® membranes were transferred to SEM sample holders

covered with conductive tape. Finally samples were sputter coated with gold–palladium (Au/Pd = 80/20; 10 nm thickness).

TEM of GO uptake into cells

BeWo cells (1×10^5 cell per insert) were grown on Transwell® membranes and 3 d post-seeding cells were exposed to GO1, s-GO and l-GO for 24 h. After exposure to GO BeWo cells were fixed in 3% glutaraldehyde in 0.1 M sodium cacodylate buffer and washed in 0.2 M sodium cacodylate buffer. After a post-fixation step in 2% osmium tetroxide in 0.1 M sodium cacodylate buffer samples were dehydrated through a graded ethanol series. Afterwards, samples were treated with acetone and finally embedded in Epon resin (Sigma-Aldrich, Buchs, Switzerland). Ultrathin sections were contrasted with 2% uranyl acetate and lead citrate (Reynolds 1963). Sections were imaged in a Zeiss EM 900 (Carl Zeiss Microscopy, GmbH, Oberkochen, Germany) at 80 kV. For each GO material (GO-1; s-GO and l-GO) two different technical replicates and multiple spots across the entire Transwell® membrane were analyzed to obtain a representative overview.

Barrier integrity

For barrier integrity studies, 1.5×10^5 BeWo cells per insert were seeded apically (Corning®, Transwell®, pore size 3.0 μm, growth area 1.12 cm^2, apical volume 0.5 ml, basolateral volume 1.5 ml; Sigma-Aldrich, Buchs, Switzerland) and cultivated for 3 d. BeWo cells were treated with 5, 10, 20 and 40 $\mu g\ ml^{-1}$ GO1, s-GO and l-GO for 6 h or 24 h (in supplemented F-12K medium). In parallel, cell layers were incubated for 15 min with 0.2% Triton X-100 (Sigma-Aldrich, Buchs, Switzerland) as positive control, cell layers without any treatment were applied as negative controls and empty membranes were used to identify the translocation capacity of the blank inserts. To detect potential influence of GO treatment on barrier integrity the transepithelial electrical resistance (TEER) was measured before and after GO treatment. In addition the exclusion capacity of the marker substance sodium fluorescein (Na–F; Sigma-Aldrich, Buchs, Switzerland), was determined after GO treatment. Inserts were washed twice with supplemented cell culture medium before TEER was measured using a chopstick electrode (STX3, World Precision Instruments Inc., Sarasota, USA). To obtain the resistance of the cell layer alone, the intrinsic TEER value (membrane without cells) was subtracted from the total TEER value measured on membranes cultivated with cells. Finally, values were corrected for the surface area ($\Omega * cm^2$). After TEER measurement the cell culture medium was replaced by 1.5 ml fresh phenol red-free RPMI-1640 medium (Sigma-Aldrich, Buchs, Switzerland) in the basolateral compartment. 0.5 ml fresh phenol red-free RPMI-1640 medium containing 5 μM Na–F was added to the apical compartment. After 4 h incubation (37 °C, 5% CO_2) translocation of Na–F was detected by fluorescence spectrometry in the basolateral samples. 50 μl of each sample was measured at 485 nm excitation and 528 emission wavelengths using a microplate reader (Mithras^2 LB 943, Berthold Technologies GmbH, Zug, Switzerland). The transferred mass (ΔQ_n) was calculated by multiplying the concentration measured at time t_n (C_n) with the well volume (V_w, 1.5 ml). Data is shown as percentages of the initial dose given to the apical chamber.

Statistical analysis

A one-way ANOVA followed by Dunnett's (MTS, LDH) or Fisher's LSD (barrier integrity) multiple comparisons test was performed to determine differences between the respective untreated control and each treatment group. An unpaired t-test (two-tailed) with Welch's correction was performed to find statistical significance between β-hCG production of each treatment group compared to the untreated control. In each cases $p < 0.05$ was considered statistically significant and GraphPad Prism version 6 was used for data analysis (GraphPad Software, La Jolla California USA, www.graphpad.com).

Results

Physicochemical properties of applied graphene oxides

To assess the potential acute toxicity of GO to human trophoblast cells, four selected GO samples from commercial (GO1, GO4) and research source (s-GO, l-GO) and with different physicochemical characteristics, especially lateral size distributions, were applied. Only non-labelled GO samples were used to exclude any potential artefacts deriving from functionalization with linkers and fluorescence dyes.

Graphene oxide sheets (s-GO and l-GO) were synthesized using a modified Hummers method (see Methods). The GO dispersions in aqueous media were homogeneous, of brownish colour, and stable at room temperature for more than 6 months. The physicochemical characterization of the GO dispersions has already been reported elsewhere [22, 41] and is summarized in figures 1(a)–(d) and in table 1. Structural properties were studied by transmission electron microscopy (TEM), and atomic force microscopy (AFM) showing that the average lateral dimensions of l-GO and s-GO are between 5–30 μm and 0.05–1 μm, respectively (figures 1(a) and (b) and table 1). Thickness of the flakes was found to be around 1-2 layers (figures 1(c) and (d) and table 1). All applied GO samples were tested for endotoxin contamination by application of the traditional LAL Gel Clot assay and Endosafe®PTS and were endotoxin free (<0.05 EU/ml).

Cell viability of BeWo cells after exposure to GO

The potential impact of GO exposure on the viability of BeWo cells was assessed by MTS assay measuring

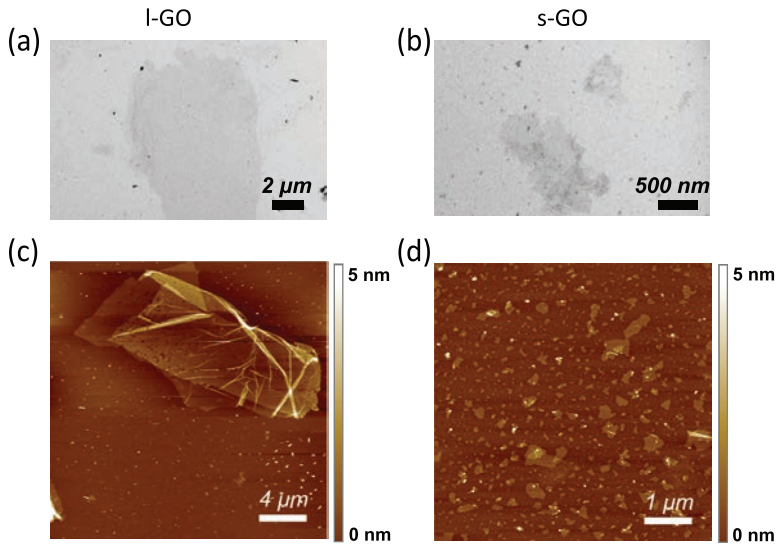

Figure 1. Physicochemical characterization of l-GO (a), (c) and s-GO (b), (d). (a) and (b) TEM micrographs of l-GO and s-GO, respectively. (c) and (d) AFM height images of l-GO and s-GO, respectively.

Table 1. Physicochemical characteristics of GO materials used in this study.

	GO1[a]	GO4[a]	s-GO (f3)	l-GO (f3)
Preparation	Modified Hummers method	Modified Hummers method	Modified Hummers method	Modified Hummers method
Starting material	Graphite	Graphite Nanofiber (GANF©)	Graflake 9580	Graflake 9580
Size distribution/lateral dimension	1–40 μm (SEM) 300–800 nm (AFM)	20 nm–1.4 μm (TEM)	0.2–1 μm (TEM) 0.05–0.5 μm (AFM)	10–30 μm (TEM) 10–15 μm (AFM)
Number of layer/thickness	0.7–1.2 nm (few to single layer)	Few to single layer	1.3 ± 0.3 nm (1–2 layers) (AFM)	1 nm (1 layer) (AFM)
Raman ID/IG ratio	1.19 ± 0.08 (633 nm) 0.96 ± 0.02 (532 nm)	0.81 ± 0.05	1.36 ± 0.03	1.33 ± 0.03
C/O ratio Zeta-potential (mV)	1.7 ± 0.1 (XPS) −39.4 ± 1.3	2.61 (XPS) −37.7 ± 0.4	2.1 (32.2%) −55.9 ± 1.4	2.1 (32.3%) −55.2 ± 1.8

[a] As reported in Kucki *et al* [21].

Abbreviations: AFM, atomic force microscopy; SEM, scanning electron microscopy; TEM, transmission electron microscopy; XPS, x-ray photoelectron spectroscopy.

the metabolic activity of the cells and by a modified LDH assay determining the number of adherent BeWo cells. For the latter, BeWo cells were lysed after GO exposure and the total amount of released lactate dehydrogenase (LDH) which is linear to the cell number was determined by LDH assay. Previous to viability assays, interference tests were conducted with all GO to ensure the absence of assay interference by the presence of GO (data not shown). To account for the unspecific absorbance of GO materials, background absorbance of residual GO was corrected on a well-to-well basis [21]. For both assays BeWo cells were exposed to GO (0–40 μg ml^{-1}) for up to 48 h. Considering deposition of GO on the cell surface due to sedimentation during 48 h incubation, applied GO concentrations would reflect a maximal exposure to 1.56 μg cm^{-2} (5 μg ml^{-1}), 3.13 μg cm^{-2} (10 μg ml^{-1}), 6.25 μg cm^{-2} (20 μg ml^{-1}) and 12.5 μg cm^{-2} (40 μg ml^{-1}) GO in case of full deposition.

In the MTS assay, GO exposure for 24 h did not alter the metabolic activity of BeWo cells. After 48 h of treatment, GO1 (5–40 μg ml^{-1}) and GO4 (40 μg ml^{-1}) but not s-GO and l-GO induced a significant decrease in mitochondrial activity (figure 2(a)). However, the number of adherent cells was not affected by the presence of all GO materials after 48 h of cultivation (figure 2(b)). Only a slight concentration-dependent decrease in the number of adherent cells was observed for GO1 and GO4 treated cells.

The absence of major acute toxicity was further supported by light microscopy observations (figure S1 (stacks.iop.org/TDM/5/035014/mmedia)). In contrast to $CdSO_4$-treated BeWo cells which exhibited concentration-dependent morphological changes and cell death, GO-exposed cells showed no obvious changes in cell morphology compared to the untreated control cells.

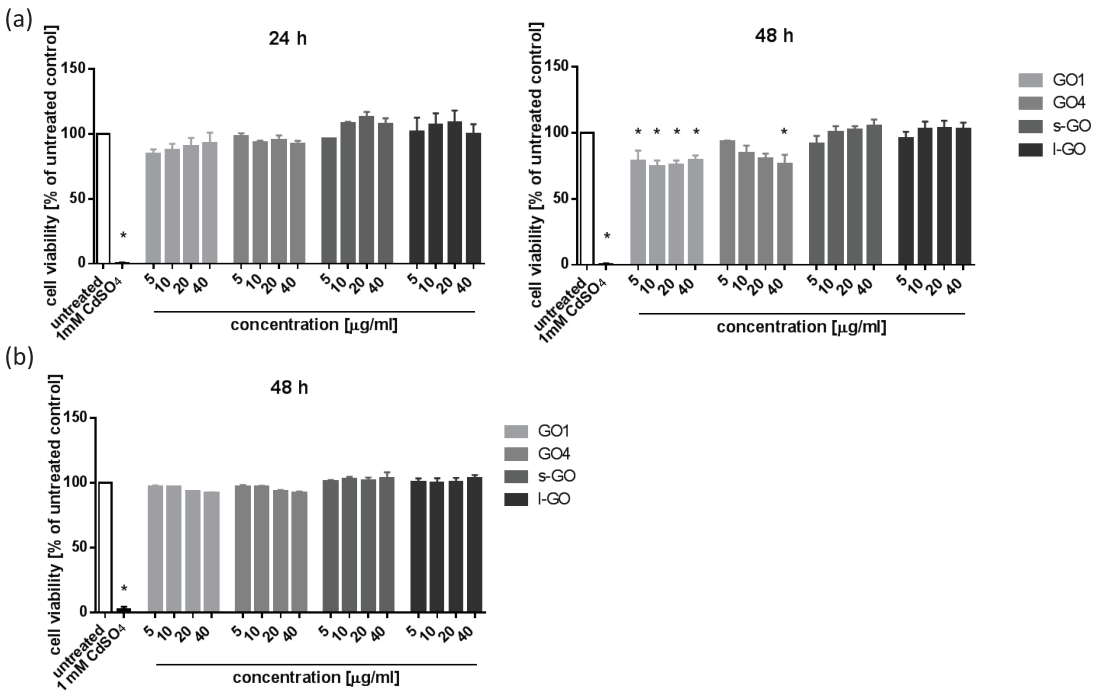

Figure 2. (a) Cell viability expressed as metabolic activity in % of control measured by MTS assay. BeWo cells were exposed to four different concentrations of GO (5–40 μg ml^{-1}) for 24 h and 48 h. (b) Total number of attached BeWo cells determined by modified LDH assay after exposure to GO (5–40 μg ml^{-1}) for 48 h and expressed as % of unexposed control cells. 1 mM $CdSO_4$ served as positive control. Data represent the mean percentages obtained from at least three independent experiments with three replicates per sample and control. Statistically significant differences are noted with * ($p < 0.05$).

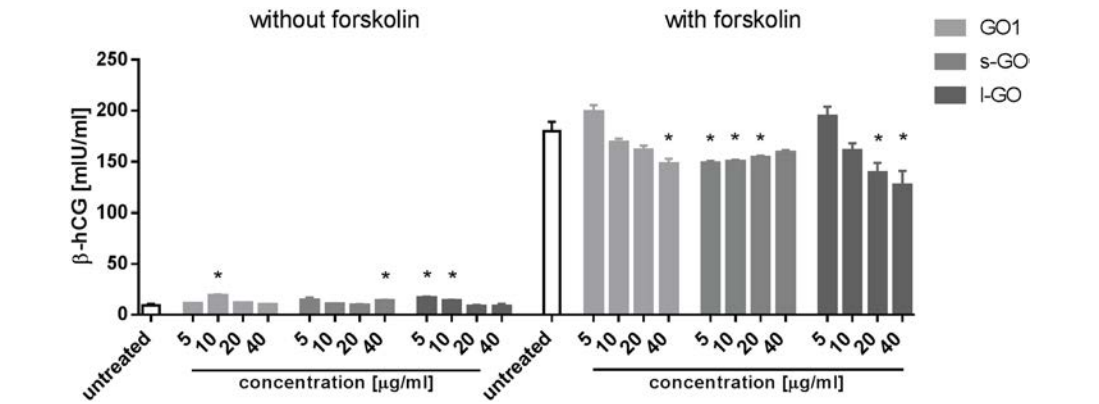

Figure 3. β-hCG production of BeWo cells with and without stimulation with 20 μM forskolin for 24 h followed by exposure to GO for another 24 h. Results are presented as M + S.E.M. of three independent experiments with four exposure replicates as well as two ELISA replicates each. Statistically significant differences are noted with * ($p < 0.05$).

Potential impact of GO exposure on the secretion of β-hCG from BeWo cells

To assess whether GO exposure might affect hormone production and release, BeWo cells were exposed to three selected GO samples: GO1 as representative for commercial GO, s-GO and l-GO to analyse the potential impact of lateral dimension. Since BeWo cells express only very low basal levels of β-hCG they were treated with 20 μM forskolin for 24 h to stimulate cell differentiation and β-hCG production, followed by exposure to four different GO concentrations (5, 10, 20 and 40 μg ml^{-1} GO) for 24 h in the absence of forskolin. Supernatants were collected and analysed by β-hCG ELISA. GO1 and l-GO induced a concentration-dependent reduction in the release of β-hCG whereas for s-GO a slight decrease in β-hCG levels was only observed at lower concentrations (figure 3). In addition, experiments with BeWo cells not stimulated with forskolin prior to GO exposure were performed to investigate whether GO can induce BeWo differentiation leading to changes in the obtained β-hCG values. In general, GO materials did not induce considerable β- hCG production in non-stimulated cells (figure 3). Small but significant differences were only detected in a concentration-independent manner for 10 μg ml^{-1} GO-1, 40 μg ml^{-1} s-GO and 5 and 10 μg ml^{-1} l-GO. Interference control experiments were performed

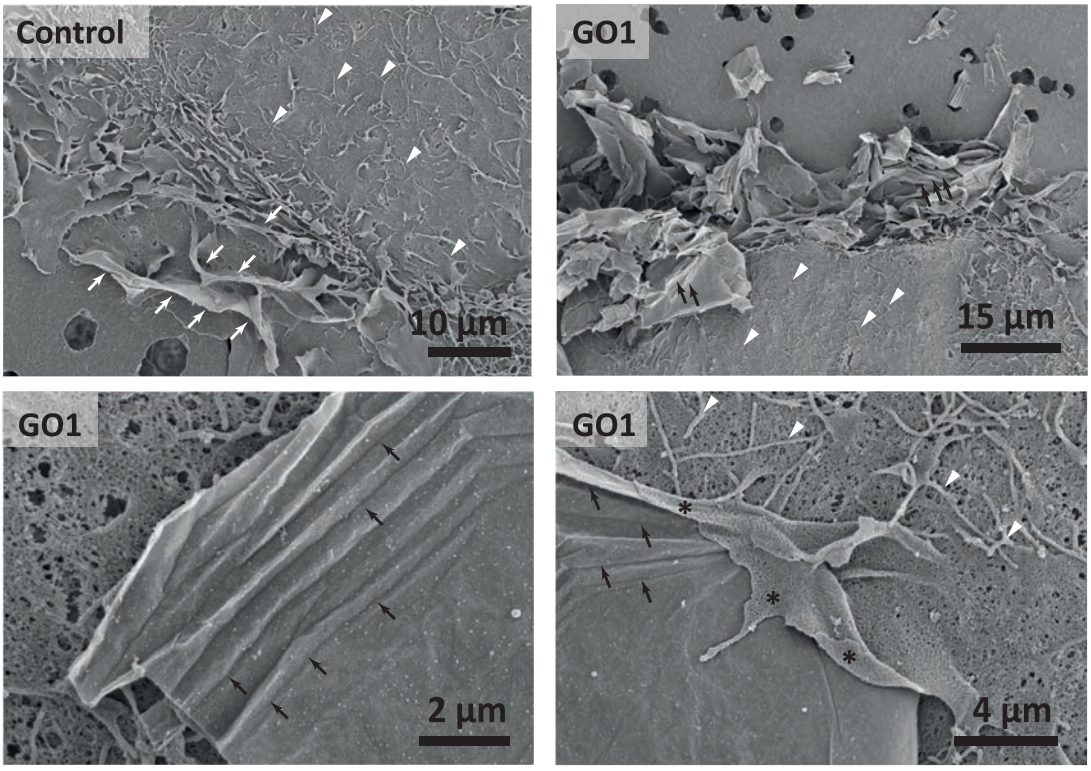

Figure 4. SEM images of the cell surface of BeWo cells grown on porous membranes. Cells were exposed to 40 μg ml^{-1} GO1 for 24 h. White arrows indicate wave like membrane structures; white arrowheads indicate microvilli; black arrows indicate fan-like GO sheets; asterisks indicate engulfment of GO sheets by membrane protrusions.

to ensure reliability of the ELISA results (data not shown).

Interaction of GO with the BeWo cell surface

As a first step to assess potential uptake of GO by placental trophoblast cells, the interaction of GO with the cell surface of BeWo cells was analysed by scanning electron microscopy (SEM) (figures 4 and 5). To assess a potential impact of the lateral size of GO on cell surface interaction and cellular uptake behavior, s-GO and l-GO were selected as they originate from the same batch preparation and exhibit similar physicochemical properties except of their lateral size distribution. GO1 was further applied as reference material confirmed to be successfully internalized by human colorectal adenocarcinoma cells (non-confluent Caco-2 cells) under comparable exposure conditions [21].

Untreated BeWo cells showed scattered apical microvilli as well as wave-like structures at the cell border similar to those observed on non-confluent Caco-2 cells [21, 42] (figures 4 and 5). Exposure to GO did not lead to marked changes in cell morphology (figures 4 and 5). All three applied GO samples showed intimate association with the Bewo cell surface. The interaction of GO1 sheets and the cell surface of BeWo cells appeared to be quite similar to those of GO1 sheets and the cell surface of non-confluent Caco-2 cells as described by Kucki *et al* [21, 42]. Highly wrinkled and folded GO1 sheets with 'concertina- or fan-like structure' were found on the BeWo cell surface (figure 4). l-GO exhibited also wrinkles and wave-like deformations of the sheets (figure 5). Nevertheless, no distinct sharp-folded sheets as observed for GO1 could be found. The mechanical properties of both GO samples seem to be significantly different with l-GO sheets appearing more flexible than GO1. s-GO formed confetti-like sheet assemblies on the cell surface as well as on the substrate (figure 5). SEM analysis gave hints towards potential uptake of GO by BeWo cells showing engulfment of GO sheets by cell protrusions (figures 4 and 5).

Analysis of GO uptake by transmission electron microscopy (TEM)

For the analysis of cellular uptake BeWo cells were grown to confluent layers on porous membranes prior to exposure with GO. After incubation with GO for 24 h, sheets of all three GO samples were internalized by the cells (figures 6–8). GO sheets were found as intracellular agglomerates without any visible surrounding plasma membrane. No signs of membrane protrusions/ruffling, endosomal tubule or autophagosome formation or other apparent morphological alterations were observed. Confluent BeWo cells were able to internalize even large GO1 sheets, similar to undifferentiated Caco-2 cells [21] (figure 6). The distinct mechanical properties of l-GO and GO1 became evident also in the TEM analysis. Whereas GO1 sheets consisted of several stacked layers and exhibited sharp bends both extra- and

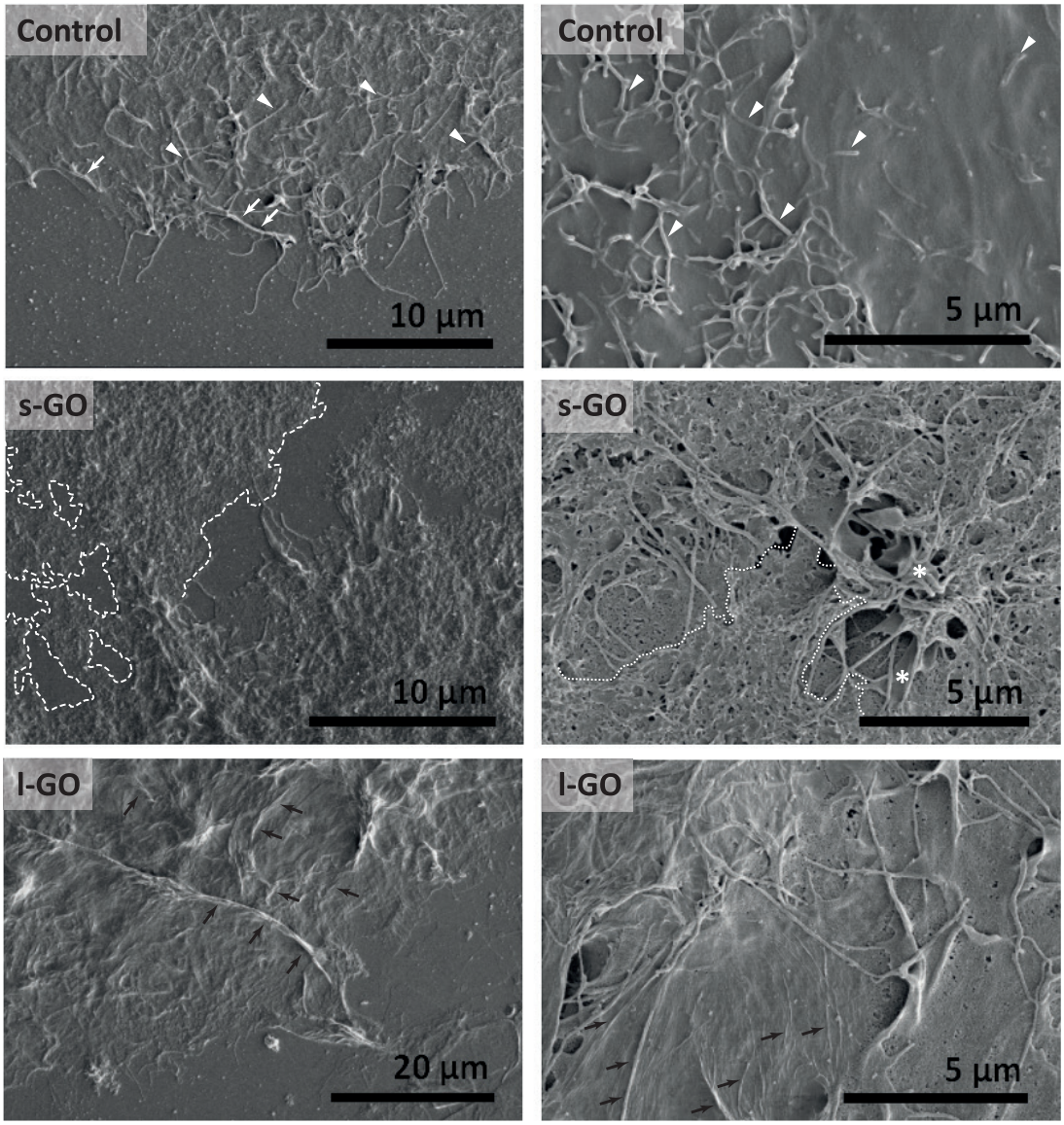

Figure 5. SEM images of the cell surface of BeWo cells grown on glass cover slides (left) or porous membranes (right). Cells were exposed to either 20 μg ml^{-1} s-GO and l-GO for 24 h. White arrows indicate wave like membrane structures; white arrowheads indicate microvilli; dashed line and dotted lines indicate the border of some s-GO sheets on the substrate or on top of the cell membrane; black arrows indicate wave-like l-GO sheets; asterisks indicate engulfment of GO sheets by membrane protrusions.

intracellularly (figure 6), l-GO formed loose and wavy agglomerates (figure 8).

Potential impact of GO on the barrier integrity of BeWo monolayers

Placental barrier integrity is of major importance for the maintenance of a healthy pregnancy. To assess whether GO can affect the passage of substances through the trophoblast layer, the permeability of BeWo cell layers grown on porous membrane supports was determined after exposure to GO for 6 and 24 h. Therefore apical to basolateral translocation of the paracellular marker Na–F was determined via fluorescence spectrometry (figure 9).

The maximum Na–F amount passing the empty membrane within 4 h was 37.3 ± 3.3% (6 h) and 38.4 ± 1.2% (24 h) of the initial dose (ID). Similar amounts were achieved after Triton X-100 treatment, which was used as positive control (6 h: 43.0 ± 4.9%; 24 h: 37.3 ± 2.1%). In presence of a BeWo cell layer, Na–F translocation was reduced to 15.7 ± 1.6% (6 h) and 14.2 ± 3.8% (24 h). Exposure of BeWo cells with GO for 6 h significantly increased Na–F translocation at 40 μg ml^{-1} GO1 and s-GO as well as 5, 20 and 40 μg ml^{-1} l-GO compared to the untreated control (25.3 ± 2.0%, 21.9 ± 1.4%, 27.1 ± 2.3%, 25.0 ± 2.8%, 28.1 ± 2.5% versus control 15.7 ± 1.6% respectively). This effect was reduced after 24 h of treatment. Only the incubation with 5 μg ml^{-1} l-GO showed a significant difference to the untreated control (26.5 ± 1.9% versus 14.2 ± 3.8%). In addition, TEER measurements were performed before and after 6 and 24 h GO exposure to identify the potential impact of GO on barrier integrity. No substantial differences of the TEER values were found when comparing the untreated control with the different treatment groups

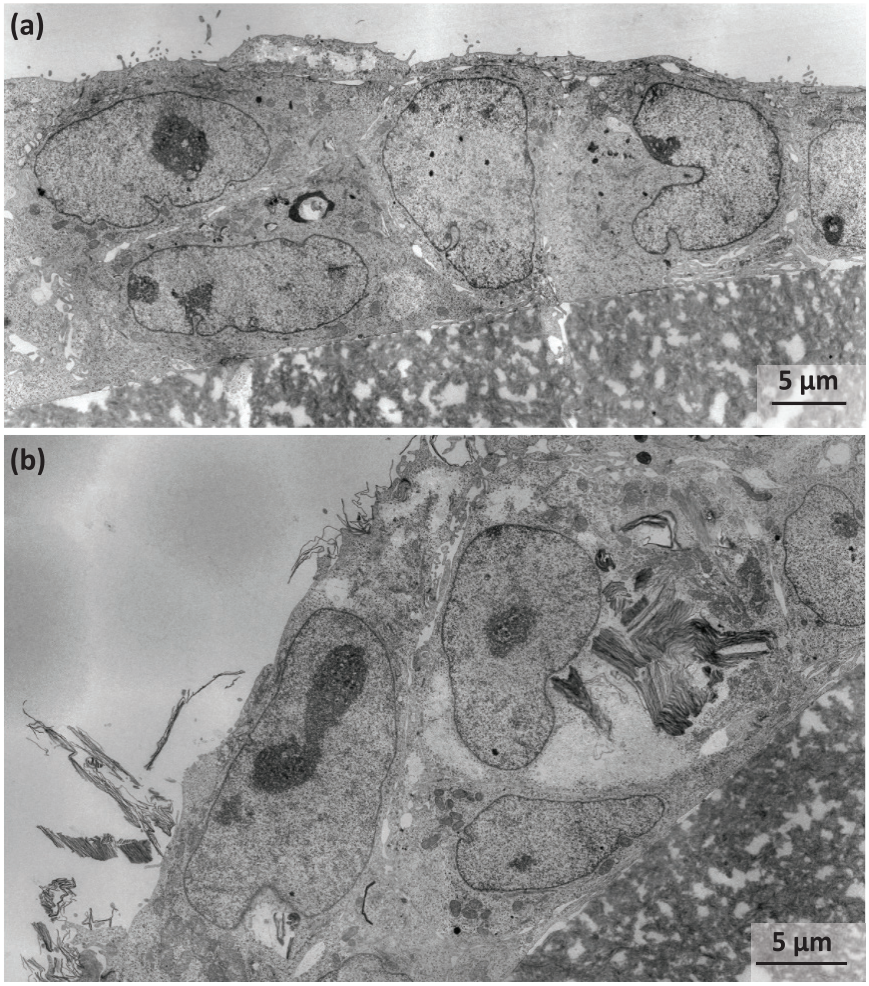

Figure 6. Compound images of TEM micrographs of BeWo cell layers with and without exposure to GO1; (a) unexposed control cells, scale bar = 5 μm; (b) cells exposed to 20 μg ml^{-1} GO1 for 24 h, scale bar = 5 μm.

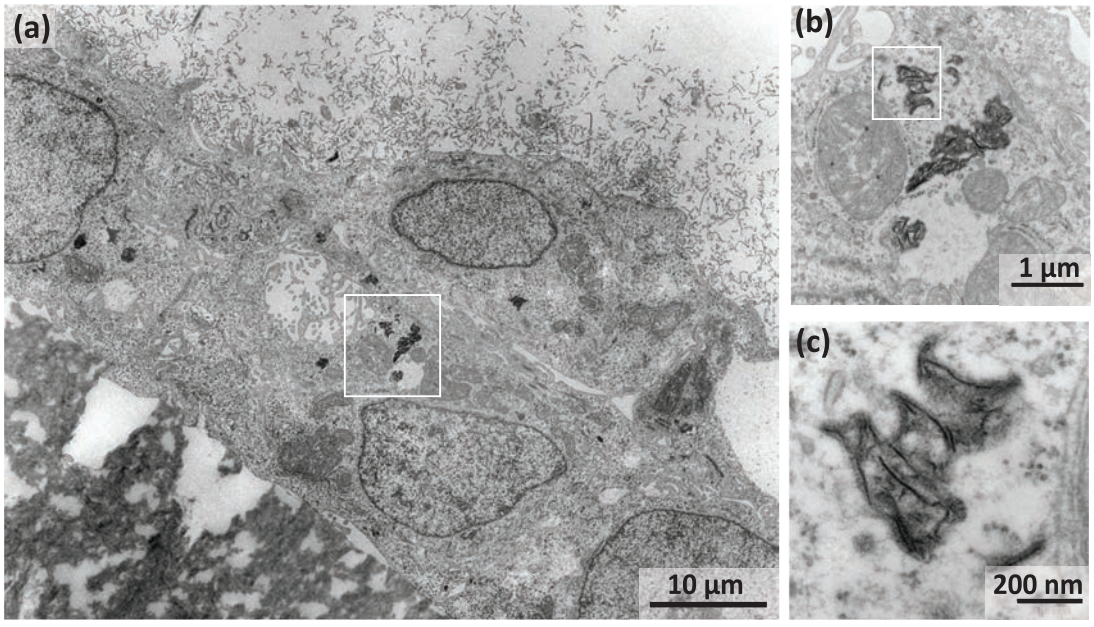

Figure 7. TEM images of BeWo cells after exposure to 20 μg ml^{-1} s-GO for 24 h. Free GO sheets are visible above the cell surface. Internalized GO sheets appear in form of aggregates. (a) Compound image of single TEM micrographs. (b) and (c) Represent enlargements of the quadrants in (a) or (b), respectively.

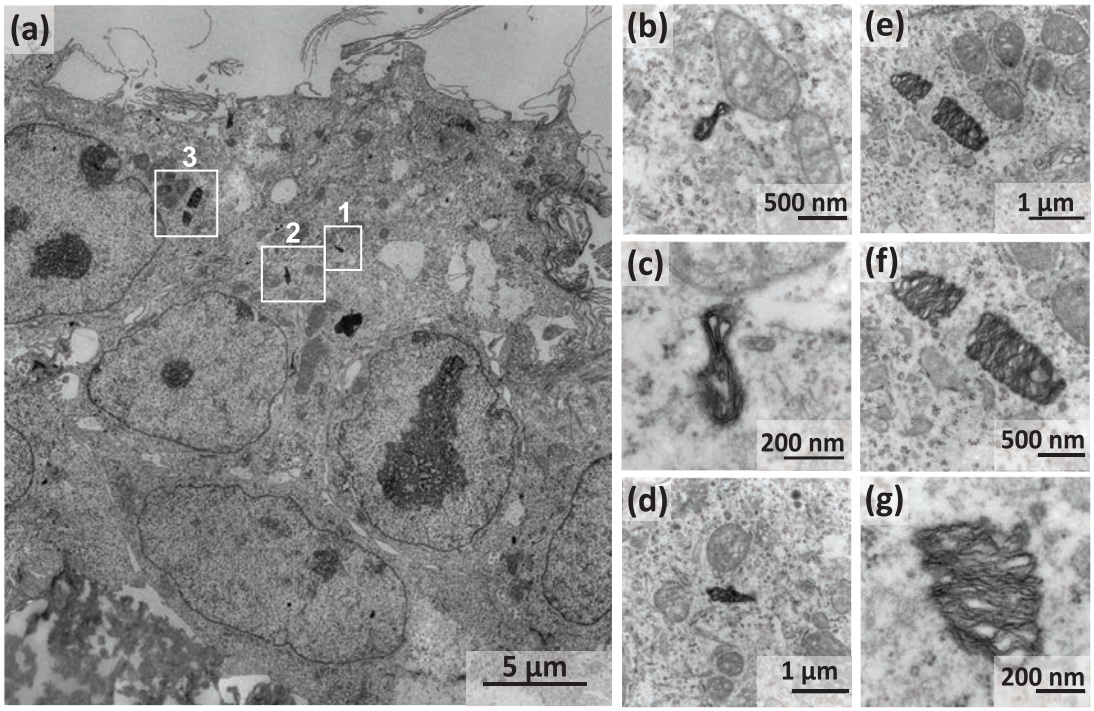

Figure 8. TEM images of BeWo cells after exposure to l-GO for 24 h. (a) Compound image of single TEM micrographs. (b)–(g) Represent enlargements of the quadrants 1, 2 or 3 in (a), respectively.

(figure S2). Only the treatment with Triton-X (positive control) resulted in a significant drop of the TEER value. Interference of the GO material with the TEER measurement was not observed (data not shown).

Discussion

Increasing development of GRM-based technologies and intended application of GRM for biomedical applications give rise to the need for assessment of their biological effects. In pregnant women GRM entering the blood circulation bear a great potential to reach the placenta as this is a highly perfused organ that is extensively exposed to circulating substances. The aim of this work was to identify whether there is reason for concern regarding acute toxicity of GO towards human placental trophoblast cells, which constitute the key cellular barrier layer and perform most of the essential placental functions. BeWo cells are widely used as a surrogate for villous cytotrophoblasts or the invasive extravillous trophoblast population. These cells exhibit several characteristics of human trophoblasts *in vivo* including the production of placental hormones or the capacity to fuse and undergo morphological and biochemical differentiation in the presence of forskolin. However, syncytialization is limited (no continuous syncytium), and due to their cancer origin, BeWo cells may not express the complete physiological receptor repertoire and endocytotic capacity. Nevertheless, BeWo cells have been successfully applied for transfer and effect studies of drugs and NPs and good correlation of the results compared to *ex vivo* placenta perfusion studies have been obtained [36, 43, 44]. Only recently, differences in NP uptake and effects have been described among first trimester placental explant cultures, primary cytotrophoblasts and BeWo cells [45]. Therefore, it will be important to carefully validate the outcome of different placenta models against human *in vivo* data to fully understand the predictive value and limitations of each model.

Amongst the plethora of industrially produced GRM, GO has probably the highest potential to reach the placental tissue in significant amounts due to its prospective medical use. Considering clinically approved drug-delivery nanocarriers with intravenous application, blood concentrations up to 100 μg ml^{-1} are conceivable (Doxil® 50 mg m^{-2} $\approx$ 18 μg ml^{-1}; Abraxane® 260 mg m^{-2} $\approx$ 94 μg ml^{-1}; AmBisome® 5 mg kg^{-1} $\approx$ 70 μg ml^{-1}; assuming a skin surface of 1.8 m^2, blood volume of 5 l and body weight of 70 kg). However, blood concentrations from occupational or consumer exposure are expected to be much lower since in general, only a low fractions of particles can pass primary tissue barriers such as the lung or intestine [46]. Exposure data on realistic pulmonary or intestinal doses of GO are lacking but for TiO_2 NPs, daily relevant doses reaching the circulation were proposed to not exceed 0.34 μg kg^{-1} BW ($\approx$5 μg ml^{-1}) [47]. To cover a potential worst-case scenario of acute GO exposure, a concentration range of 5–40 μg ml^{-1} was applied to BeWo trophoblast cells for up to 48 h.

All applied GO did not induce any apparent morphological alterations or cell death of BeWo cells at concentrations up to 40 μg ml^{-1}. Nevertheless, it is crucial to also exclude potential adverse effects of GO on proper functionality of the cells. For instance, it has

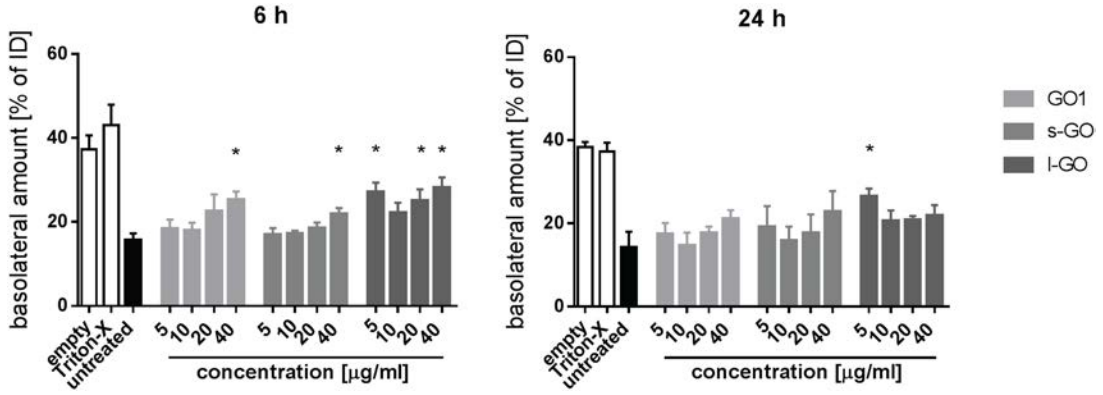

Figure 9. Transport of Na–F across the BeWo layer after 6 h and 24 h of GO treatment. BeWo cells were grown for 3 d before treatment of the cell layers for 6 or 24 h with 5, 10, 20 and 40 μg ml^{-1} GO1, s-GO and l-GO, respectively. Then 5 μM Na–F was added to the apical chamber and its concentration was determined in the basolateral compartment after 4 h incubation (37 °C/5% CO_2). Cell free inserts (empty) and the positive control Triton X-100 were used to determine the maximal translocation across the membrane. Results from 3 independent biological experiments are presented as M + S.E.M. Statistically significant differences are noted with * ($p < 0.05$).

recently been shown that GO significantly inhibits cell growth at sublethal concentrations by causing extracellular iron deficiency [48]. Here, some of the GO materials slightly decreased the metabolic activity of the cells which may have long-term consequences on placental function and viability. A highly important function of the human placenta is the production of a large variety of hormones to maintain pregnancy and ensure proper fetal growth. Due to its pleiotropic functions, hCG is frequently used as a marker to assess the functionality of trophoblasts and placental tissue after exposure to xenobiotics. All tested GO did reduce β-hCG secretion which could result in pregnancy disorders such as preeclampsia, intrauterine growth restriction or miscarriage [49, 50]. Another key function of the human placental barrier is to prevent translocation of xenobiotics as well as pathogens. Therefore assessment of the potential impact of GO on the placental barrier integrity is of major importance. Recently it was shown that micrometer-sized GO (mGO) can interact with the cell membrane of MCF-7 cells (human breast cancer cell line) and enhance its permeability [51]. In detail, the results indicate that the applied mGO material was interacting with aquaporines in the cells and that an enhanced water efflux could be used for increased drug delivery of small compounds across cell barriers that contain these channels. Aquaporines are also present in the syncytiotrophoblast of the human placenta regulating the materno-fetal transcellular transport of water and solutes [52]. However, studies showed that the expression of these proteins is modified in problematic placental conditions such as pre-eclampsia and that they seem to have versatile functions beside water transport [53, 54]. Here, we investigated if the applied GO materials are able to enhance cell permeability at the placental barrier *in vitro* using the BeWo transfer model [37, 55, 56]. To determine the potential effect of GO on BeWo barrier integrity, the translocation of the model substance sodium fluoresceine (Na–F) was determined following 6 and 24 h of GO treatment. Na–F was used previously as marker substance for passive paracellular transport *in vitro* [57]. Lately it was also demonstrated that Na–F acts as substrate for organic anion transporting polypeptides (OATP) [58]. These transporters are present *in vivo* and in BeWo cells [59–61]. GO exposure resulted in a transient increase of Na–F translocation across the BeWo trophoblast barrier supporting the previously formulated hypothesis that GO may increase barrier permeability [51]. However, the observed leakiness of the BeWo layer was not reflected by a drop in the TEER values. The high deviations observed between individual measurements may prohibit detecting more subtle alterations in barrier integrity. Interestingly, a similar effect has been described in a recent *in vivo* study, where intravenous injection of reduced GO (rGO) induced a transient opening of the blood-brain barrier [62]. Although the concomitant increase in penetration of Evans blue dye and lanthanum nitrate infiltration as well as down-regulation of tight junction, adhesion junction and basement membrane proteins indicates a weakening of the paracellular pathway, the exact mechanisms how GO affects barrier tightness remain to be elucidated.

Ultrastructural analysis of GO uptake by BeWo cells revealed that all GO materials did closely associate with the cell surface and were effectively internalized by the cells despite of their large sizes. Therefore it is conceivable that GO may interfere with intra- and/or extracellular molecules and pathways. Further investigations to address if GO can pass the trophoblast barrier and potentially reach the fetal circulation were not possible in the BeWo transfer model due to the presence of the artificial membrane support as already discussed in a recent review [3]. 2D materials with lateral dimensions in the micrometer range as well as 2D material aggregates will be retained and not able to pass the membrane pores. Alternative advanced pla-

centa models such as 3D placental microtissues [63] or the *ex vivo* placenta perfusion model [64] might be better suited to address penetration and/or transfer of GO but will require highly sensitive analytical technologies and/or labelled GO materials to reliably detect translocated particles.

Finally, it will be indispensable to gain mechanistic insights how GO physicochemical properties impact biological effects to support the safe design of GO for industrial, commercial and medical applications. Despite the often reported size-dependent effects of GO sheets, we did not see any clear correlation of GO lateral sizes on the observed biological responses. For instance, s-GO and l-GO having the same origin but different lateral size distribution showed virtually no effects on cell viability at applied GO concentrations. However, GO1 and GO4 induced a slight decrease in mitochondrial activity which might be explained by the difference in layer number and thickness of the GO sheet assemblies resulting in distinct mechanical properties. In electron microscopy analysis l-GO appeared as wave-like sheets, whereas GO1 formed sharp-edged fan-like structures with apparently higher layer number. Higher flexibility can facilitate cellular uptake and intracellular packing of GRM, whereas more rigid structures impede these processes. The importance of the mechanical properties in respect to biological responses was already discussed by Sanchez *et al* [65]. In addition a recent study highlighted the potential relevance of the mechanical properties for the cellular uptake of GO by non-confluent Caco-2 cells [42].

Conclusions

Our *in vitro* results did not reveal major acute cytotoxicity of different GO towards placental trophoblasts which constitute the key cell type of the placenta mediating selective transport, barrier, endocrine, metabolic and immunological functions. However, we did observe a slight decrease in mitochondrial activity and hCG secretion as well as the internalization of even large GO sheets in BeWo cells. Therefore it will be central to understand if placental accumulation and the observed interferences with trophoblast functionality (e.g. barrier and endocrine function) may have long term consequences on maternal and/or fetal health. Future studies verifying the observed effects in more complex placental models (e.g. human placental microtissues or explant cultures, human *ex vivo* placenta perfusion, *in vivo* studies) and clarifying the underlying mechanisms are expected to support the sustainable use and safe design of GO for various applications and the regulation of GO exposure during pregnancy.

Furthermore, we confirmed the previous observation from the blood-brain barrier that GO can induce a transient increase in barrier permeability also at the placental epithelial trophoblast barrier. This suggests that transient barrier opening might be a universal feature of GO, applicable to any epithelial tissue barrier. If true, GO may be an interesting candidate to enhance the delivery of impermeable drugs across biological barriers given that their safety can be proven.

Acknowledgment

The research leading to these results has received funding from the European Union (EU) Seventh Framework Programme Graphene Flagship project (grant agreement n°604391) and the EU Horizon 2020 Framework Graphene Flagship project GrapheneCore1 (grant agreement n°696656). Additional financial support was given by the BMBF-project NanoUmwelt (03X0150). We thank Grupo Antolin, Spain for providing graphene oxide (GO4). LN would like to acknowledge a studentship from the EPSRC - North West Nanoscience Doctoral Training Centre (NOWNANO DTC; EP/G03737X/1). The authors would like to acknowledge Dr Neus Lozano Valdes for the production of s-GO (f3) and l-GO (f3).

Conflicts of interest

The authors declare no conflict of interest.

ORCID iDs

Melanie Kucki https://orcid.org/0000-0001-7502-6334
Leonie Aengenheister https://orcid.org/0000-0003-2195-6602
Sandra Vranic https://orcid.org/0000-0002-6653-7156
Leon Newman https://orcid.org/0000-0003-2099-2660
Ester Vazquez https://orcid.org/0000-0003-3223-8024
Kostas Kostarelos https://orcid.org/0000-0002-2224-6672
Peter Wick https://orcid.org/0000-0002-0079-4344
Tina Buerki-Thurnherr https://orcid.org/0000-0003-3723-6562

References

[1] Pelaz B *et al* 2017 Diverse applications of nanomedicine *ACS Nano* **11** 2313–81
[2] Keelan J A, Leong J W, Ho D and Iyer K S 2015 Therapeutic and safety considerations of nanoparticle-mediated drug delivery in pregnancy *Nanomedicine* **10** 2229–47
[3] Muoth C, Aengenheister L, Kucki M, Wick P and Buerki-Thurnherr T 2016 Nanoparticle transport across the placental barrier: pushing the field forward! *Nanomedicine* **11** 941–57
[4] Blum J L, Xiong J Q, Hoffman C and Zelikoff J T 2012 Cadmium associated with inhaled cadmium oxide nanoparticles impacts fetal and neonatal development and growth *Toxicol. Sci.* **126** 478–86

[5] Campagnolo L et al 2013 Biodistribution and toxicity of pegylated single wall carbon nanotubes in pregnant mice *Part. Fibre Toxicol.* **10** 21
[6] Paul E et al 2017 Pulmonary exposure to metallic nanomaterials during pregnancy irreversibly impairs lung development of the offspring *Nanotoxicology* **11** 484–95
[7] Philbrook N A, Walker V K, Afrooz A R M N, Saleh N B and Winn L M 2011 Investigating the effects of functionalized carbon nanotubes on reproduction and development in Drosophila melanogaster and CD-1 mice *Reprod. Toxicol.* **32** 442–8
[8] Zalgeviciene V et al 2017 Quantum dots mediated embryotoxicity via placental damage *Reprod. Toxicol.* **73** 222–31
[9] Kurapati R, Kostarelos K, Prato M and Bianco A 2016 Biomedical uses for 2D materials beyond graphene: current advances and challenges ahead *Adv. Mater.* **28** 6052–74
[10] Jasim D A, Menard-Moyon C, Begin D, Bianco A and Kostarelos K 2015 Tissue distribution and urinary excretion of intravenously administered chemically functionalized graphene oxide sheets *Chem. Sci.* **6** 3952–64
[11] Chung C, Kim Y-K, Shin D, Ryoo S-R, Hong B H and Min D-H 2013 Biomedical applications of graphene and graphene oxide *Acc. Chem. Res.* **46** 2211–24
[12] Kostarelos K and Novoselov K S 2014 Graphene devices for life *Nat. Nanotechnol.* **9** 744–5
[13] Kostarelos K and Novoselov K S 2014 Materials science. Exploring the interface of graphene and biology *Science* **344** 261–3
[14] Servant A, Bianco A, Prato M and Kostarelos K 2014 Graphene for multi-functional synthetic biology: the last 'zeitgeist' in nanomedicine *Bioorg. Med. Chem. Lett.* **24** 1638–49
[15] Kostarelos K 2016 Translating graphene and 2D materials into medicine *Nat. Rev. Mater.* **1** 16084
[16] Bitounis D, Ali-Boucetta H, Hong B H, Min D-H and Kostarelos K 2013 Prospects and challenges of graphene in biomedical applications *Adv. Mater.* **25** 2258–68
[17] Zhang Y, Nayak T R, Hong H and Cai W 2012 Graphene: a versatile nanoplatform for biomedical applications *Nanoscale* **4** 3833
[18] Orecchioni M, Cabizza R, Bianco A and Delogu L G 2015 Graphene as cancer theranostic tool: progress and future challenges *Theranostics* **5** 710–23
[19] Liu Z, Robinson J T, Sun X and Dai H 2008 PEGylated nanographene oxide for delivery of water-insoluble cancer drugs *J. Am. Chem. Soc.* **130** 10876–7
[20] Chang Y et al 2011 *In vitro* toxicity evaluation of graphene oxide on A549 cells *Toxicol. Lett.* **200** 201–10
[21] Kucki M et al 2016 Interaction of graphene-related materials with human intestinal cells: an *in vitro* approach *Nanoscale* **8** 8749–60
[22] Mukherjee S P et al 2016 Detection of endotoxin contamination of graphene based materials using the TNF-alpha expression test and guidelines for endotoxin-free graphene oxide production *PloS One* **11** e0166816
[23] Kiew S F, Kiew L V, Lee H B, Imae T and Chung L Y 2016 Assessing biocompatibility of graphene oxide-based nanocarriers: a review *J. Control. Rel.* 217–28
[24] Pietroiusti A et al 2011 Low doses of pristine and oxidized single-wall carbon nanotubes affect mammalian embryonic development *ACS Nano* **5** 4624–33
[25] Qi W et al 2014 Damaging effects of multi-walled carbon nanotubes on pregnant mice with different pregnancy times *Sci. Rep.* **4** 4352
[26] Huang X et al 2014 The genotype-dependent influence of functionalized multiwalled carbon nanotubes on fetal development *Biomaterials* **35** 856–65
[27] Xu S, Zhang Z and Chu M 2015 Long-term toxicity of reduced graphene oxide nanosheets: effects on female mouse reproductive ability and offspring development *Biomaterials* **54** 188–200
[28] Dilworth M R and Sibley C P 2013 Review: transport across the placenta of mice and women *Placenta* **34** S34–9
[29] Enders A C and Blankenship T N 1999 Comparative placental structure *Adv. Drug Deliv. Rev.* **38** 3–15
[30] Schmidt A, Morales-Prieto D M, Pastuschek J, Frohlich K and Markert U R 2015 Only humans have human placentas: molecular differences between mice and humans *J. Reprod. Immunol.* **108** 65–71
[31] Feneley M R and Burton G J 1991 Villous composition and membrane thickness in the human placenta at term: a stereological study using unbiased estimators and optimal fixation techniques *Placenta* **12** 131–42
[32] Jones C J, Harris L K, Whittingham J, Aplin J D and Mayhew T M 2008 A re-appraisal of the morphophenotype and basal lamina coverage of cytotrophoblasts in human term placenta *Placenta* **29** 215–9
[33] Pattillo R A and Gey G O 1968 The establishment of a cell line of human hormone-synthesizing trophoblastic cells *in vitro* *Cancer Res.* **28** 1231–6
[34] Pattillo R A, Gey G O, Delfs E and Mattingly R F 1968 Human hormone production *in vitro* *Science* **159** 1467–9
[35] Pattillo R A et al 1971 The hormone-synthesizing trophoblastic cell *in vitro*: a model for cancer research and placental hormone synthesis *Ann. New York Acad. Sci.* **172** 288–98
[36] Poulsen M S, Rytting E, Mose T and Knudsen L E 2009 Modeling placental transport: correlation of *in vitro* BeWo cell permeability and *ex vivo* human placental perfusion *Toxicol. In Vitro* **23** 1380–6
[37] Bode C J, Jin H, Rytting E, Silverstein P S, Young A M and Audus K L 2006 *In vitro* models for studying trophoblast transcellular transport *Methods Mol. Med.* **122** 225–39
[38] Ali-Boucetta H, Bitounis D, Raveendran-Nair R, Servant A, Van den Bossche J and Kostarelos K 2013 Purified graphene oxide dispersions lack *in vitro* cytotoxicity and *in vivo* pathogenicity *Adv. Healthc. Mater.* **2** 433–41
[39] Dhifaf A J, Neus L and Kostas K 2016 Synthesis of few-layered, high-purity graphene oxide sheets from different graphite sources for biology *2D Mater.* **3** 014006
[40] Kucki M 2012 NanoKon SOP 2.2.2: Detection and Semi-Quantification of Endotoxin Contaminations in Nanoparticle Suspensions2012 (http://nanopartikel.info/files/methodik/SOPs_aus_Projekten/NanoKon_SOP-2-2-2.pdf)
[41] Rauti R et al 2016 Graphene oxide nanosheets reshape synaptic function in cultured brain networks *ACS Nano* **10** 4459–71
[42] Kucki M et al 2017 Uptake of label-free graphene oxide by Caco-2 cells is dependent on the cell differentiation status *J. Nanobiotechnol.* **15** 46
[43] Li H, van Ravenzwaay B, Rietjens I M and Louisse J 2013 Assessment of an *in vitro* transport model using BeWo b30 cells to predict placental transfer of compounds *Arch. Toxicol.* **87** 1661–9
[44] Poulsen M S, Mose T, Maroun L L, Mathiesen L, Knudsen L E and Rytting E 2015 Kinetics of silica nanoparticles in the human placenta *Nanotoxicology* **9** 79–86
[45] Juch H et al 2018 Dendritic polyglycerol nanoparticles show charge dependent bio-distribution in early human placental explants and reduce hCG secretion *Nanotoxicology* **12** 90–103
[46] Kreyling W G, Semmler-Behnke M, Takenaka S and Möller W 2013 Differences in the biokinetics of inhaled nano- versus micrometer-sized particles *Acc. Chem. Res.* **46** 714–22
[47] Kreyling W G et al 2017 Quantitative biokinetics of titanium dioxide nanoparticles after intravenous injection in rats: part 1 *Nanotoxicology* **11** 434–42
[48] Yu Q et al 2017 Graphene oxide significantly inhibits cell growth at sublethal concentrations by causing extracellular iron deficiency *Nanotoxicology* **11** 1102–14
[49] Korevaar T I M et al 2016 The risk of preeclampsia according to high thyroid function in pregnancy differs by hCG concentration *J. Clin. Endocrinol. Metab.* **101** 5037–43
[50] Norris W, Nevers T, Sharma S and Kalkunte S 2011 Review: hCG, preeclampsia and regulatory T cells *Placenta* **32** S182–5
[51] Wu C et al 2015 Vacuolization in cytoplasm and cell membrane permeability enhancement triggered by micrometer-sized graphene oxide *ACS Nano* **9** 7913–24

[52] Damiano A, Zotta E, Goldstein J, Reisin I and Ibarra C 2001 Water channel proteins AQP3 and AQP9 are present in syncytiotrophoblast of human term placenta *Placenta* **22** 776–81
[53] Szpilbarg N *et al* 2016 Placental programmed cell death: insights into the role of aquaporins *MHR Basic Sci. Reprod. Med.* **22** 46–56
[54] Damiano A E, Zotta E and Ibarra C 2006 Functional and molecular expression of AQP9 channel and UT-A transporter in normal and preeclamptic human placentas *Placenta* **27** 1073–81
[55] Cartwright L *et al* 2012 *In vitro* placental model optimization for nanoparticle transport studies *Int. J. Nanomed.* **7** 497–510
[56] Liu F, Soares M J and Audus K L 1997 Permeability properties of monolayers of the human trophoblast cell line BeWo *Am. J. Physiol.* **273** C1596–604
[57] Levkovitz R, Zaretsky U, Jaffa A J, Hod M and Elad D 2013 *In vitro* simulation of placental transport: part II. Glucose transfer across the placental barrier model *Placenta* **34** 708–15
[58] Nabekura T, Kawasaki T, Kamiya Y and Uwai Y 2015 Effects of antiviral drugs on organic anion transport in human placental BeWo cells *Antimicrobial Agents Chemother.* **59** 7666–70
[59] Briz O, Serrano M A, MacIas R I R, Gonzalez-Gallego J and Marin J J G 2003 Role of organic anion-transporting polypeptides, OATP-A, OATP-C and OATP-8, in the human placenta-maternal liver tandem excretory pathway for foetal bilirubin *Biochem. J.* **371** 897–905
[60] Sato K *et al* 2003 Expression of organic anion transporting polypeptide E (OATP-E) in human placenta *Placenta* **24** 144–8
[61] Ugele B, St-Pierre M V, Pihusch M, Bahn A and Hantschmann P 2003 Characterization and identification of steroid sulfate transporters of human placenta *Am. J. Physiol.* **284** E390–8
[62] Mendonça M C P *et al* 2015 Reduced graphene oxide induces transient blood–brain barrier opening: an *in vivo* study *J. Nanobiotechnol.* **13** 78
[63] Muoth C *et al* 2016 A 3D co-culture microtissue model of the human placenta for nanotoxicity assessment *Nanoscale* **8** 17322–32
[64] Grafmueller S, Manser P, Krug H F, Wick P and von Mandach U 2013 Determination of the transport rate of xenobiotics and nanomaterials across the placenta using the *ex vivo* human placental perfusion *Model. J Vis Exp.* **76** e50401
[65] Sanchez V C, Jachak A, Hurt R H and Kane A B 2012 Biological interactions of graphene-family nanomaterials: an interdisciplinary review *Chem. Res. Toxicol.* **25** 15–34